Coupling between meniscus and smectic-*A* films: Circular and catenoid profiles, induced stress, and dislocation dynamics

Frédéric Picano,[1] Robert Hołyst,[1,2] and P. Oswald[1]
[1]*Laboratoire de Physique de l'Ecole Normale Supérieure de Lyon, 69364 Lyon Cedex 07, France*
[2]*Institute of Physical Chemistry PAS and College of Science, Department III, Kasprzaka 44/52, 01224 Warsaw, Poland*
(Received 24 November 1999; revised manuscript received 31 May 2000)

In this paper we discuss the formation and shape of the meniscus between a free-standing film of a smectic-*A* phase and a wall (in practice the frame that supports the film). The wall may be flat or circular, and the system with or without a reservoir of particles. The formation of the meniscus is always an irreversible thermodynamic process, since it involves the creation of dislocations in the bulk (therefore it involves friction). The four basic shapes of meniscus discussed are the following: exponential, algebraic ($x^{3/2}$), circular, and catenoid. Three principal regions of the whole meniscus must be distinguished: close to the wall with a high density of dislocations, away from the wall with medium density of dislocations, and far from the wall (i.e., close to the film) with a low density of dislocations (vicinal regime). The region with medium density of dislocations is observable using a microscope, and is determined by the competition between surface tension, energy of dislocations, and pressure difference set by the mass of the meniscus or by the reservoir. Its profile is circular as observed in recent experiments [J.-C. Géminard, R. Hołyst, and P. Oswald, Phys. Rev. Lett. **78**, 1924 (1997)]. By contrast, the vicinal regime with low density of dislocations is never observable with an optical microscope. In the regime with a high density of dislocations, the reasons why the dislocations tend to gather by forming giant dislocations and rows of focal conics are discussed. Finally, we discuss the stability of a smectic film with respect to the formation of a dislocation loop. We show experimentally that the critical radius of the loop is proportional to the curvature radius of the meniscus in its circular part, in agreement with the theory. In addition, we show that the mobility of edge dislocations measured in thick films is in agreement with that found in bulk samples from a creep experiment. This result confirms again our model of the meniscus.

PACS number(s): 61.30.Eb, 61.30.Jf, 68.10.−m

I. INTRODUCTION

The size of the meniscus in ordinary liquids is set by the capillary length [1]

$$l_c = \left(\frac{\gamma_{LA}}{\rho g} \right)^{1/2}, \tag{1.1}$$

which reflects the competition between the gravity and the surface tension in the creation of the meniscus. Here γ_{LA} is the liquid-air surface tension, ρ is the liquid density, and g is the gravitational acceleration. The height of the meniscus at the wall h_0 is set by the competition between the capillarity forces and the gravity [Fig. 1(a)],

$$h_0 = \left(2 \frac{\gamma_{LA}(1-\sin\theta)}{\rho g} \right)^{1/2}, \tag{1.2}$$

and θ is a contact angle at the wall given by

$$\cos\theta = \frac{\gamma_{WA} - \gamma_{WL}}{\gamma_{LA}}. \tag{1.3}$$

The following surface tensions appear: γ_{LA}, γ_{WL}, and γ_{WA}, where *W* stands for wall, *L* for liquid, and *A* for air. Taking typical values we find that the horizontal size of the meniscus is of the order of 0.2 cm, and that is why we can see it easily. Far away from the wall, located at $x=0$, the meniscus has the exponential form

$$h(x) = h_0 \exp(-x/l_c). \tag{1.4}$$

The experiments performed on smectic liquid crystal films give completely different results [2]. First of all the size of the smectic meniscus may be about two orders of magnitude smaller than the simple estimate based on the capillary length given by Eq. (1.2). Moreover, its shape is circular and not exponential. These observations called for some theoretical explanation, and it is the purpose of this paper to describe the formation of smectic meniscus and to describe the differences between simple liquids and smectic-*A* liquid crystals. As far as we know the problem of formation of a meniscus in complex liquids has just started to be studied [2,3].

The paper is organized as follows. In Sec. II we discuss the main differences between the formation of a smectic meniscus and a meniscus in ordinary liquids. In Sec. III we derive the form of the meniscus for smectic liquid crystals near a flat wall. In Sec. IV we discuss the stability of a smectic film with respect to the formation of a dislocation loop, and we show that our theoretical model is in agreement with the experiment.

II. FORMATION OF A MENISCUS IN SMECTICS

Molecules in smectic-*A* liquid crystal are arranged in liquidlike layers parallel to each other. The distance between the layers $d \approx 30$ Å is set by the length l of the liquid crystalline molecules ($l \leqslant d \leqslant 2l$). Dislocations, known from the theory of solid structure [4], also appear in smectic liquid

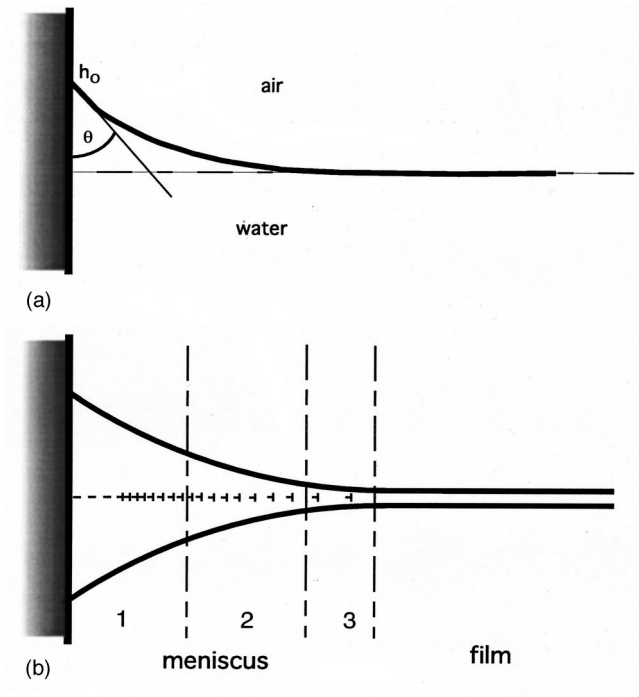

FIG. 1. Schematic representation of the water-air meniscus near a vertical wall (a), and of the meniscus between a smectic film and a vertical wall (b). Regions (1)–(3) are defined in the text.

crystals [5–8]. If we want to change the number of layers in a monodomain of a smectic sample, we have to nucleate elementary edge dislocations. An elementary dislocation changes the number of layers of the sample by one; in principle one can have edge dislocations that change the number of layers by more than one layer. The nucleation of dislocations has a clear implication for the formation of the meniscus that forms between a free-standing film and its support, namely, the height of the meniscus depends on the process of its creation, i.e., on the number of dislocations created during the process. If the number of dislocations in the meniscus is N, its height at the wall is fixed, and is equal to Nd. Here we assume that the smectic layers are perpendicular to the vertical wall of the frame.

In simple liquids, the height of the meniscus given by Eqs. (1.2) and (1.3) does not depend on the process which leads to its creation, while in smectic liquid crystals the height is fixed by the process. Because the energy barrier for the creation of an edge dislocation is usually much greater than the thermal energy, the capillary forces do not play any role in determining the meniscus height. This is the first clear difference between simple liquids and smectic liquid crystals.

Needless to say, the creation of the meniscus in an ordinary liquid can be obtained in a reversible process. In a smectic this is not true, and any process leading to the creation of the meniscus is irreversible. This is due to the necessity to nucleate dislocations.

It is therefore obvious that in an ordinary liquid the final state of the meniscus will be always the same irrespective of the particular process leading to its creation. This is not true in smectics, where different processes may lead to different final states. In one process we may create N dislocations, and in the other $N+1$, and, although we may reach the same thermodynamic state, the meniscus will be different in these two cases.

Another difference between ordinary liquids and smectics is more subtle, yet it determines the shape of the smectic meniscus and explains the metastability of the films. Indeed, it is common knowledge that, due to mechanical equilibrium, an isotropic liquid in contact with air must have the same pressure as the air if its interface is flat. However, this does not have to be so in a smectic-A liquid crystal, because its layers are elastic and can support a normal elastic stress. This stress σ can equilibrate any pressure difference $\Delta p = p_{\rm air} - p_{\rm smectic}$ imposed by the meniscus, providing it is not too large (this point will discussed below). This remark is crucial for understanding the *metastability* of smectic free-standing films where we know that the number m of layers can be experimentally controlled one by one from m very large down to $m=2$ [9,10]. It also explains why the film tension τ linearly depends on its thickness $H=md$,

$$\tau = 2\gamma_{SA} + \Delta p H, \tag{2.1}$$

where γ_{SA} is the surface free energy of the smectic-air interface. This law has was found experimentally in Refs. [9, 11]. Finally, the stress will be permanent in the film if the system is not coupled to a reservoir of particles at the same pressure as $p_{\rm air}$, with a value directly related to the total volume of the meniscus. More precisely, we will show in Sec. III that the meniscus profile is essentially circular [2] (of radius R) close to the film, and that the stress $\sigma = -\Delta p$ is related to R via the Laplace law

$$R = \frac{\gamma_{SA}}{\Delta p}. \tag{2.2}$$

It is important to note that the elastic stress σ vanishes on average inside the meniscus because the dislocations (which we know to be repulsed by free surfaces in smectic-A phases [12]) can climb parallel to the layers to relax the stress. We also emphasize that all these results are true providing that we neglect the elastic interactions between dislocations, which we know to be true when they are located in the same plane [7,8]. Below, we discuss the meniscus shape in more details.

III. SHAPE OF THE SMECTIC MENISCUS NEAR A FLAT WALL

Let us assume that we have a flat wall in contact with the smectic. The z axis is along the wall, and the x axis is perpendicular to the wall.

In smectic-A liquid crystals, we distinguish three principal regions of the whole meniscus [Fig. 1(b)]: close to the wall with a high density of dislocations, away from the wall with a medium density of dislocations, and far from the wall (i.e., close to the film) with a low density of dislocations. In the first region (the least known) the dislocations group together to form giant dislocations of very large Burgers vectors (up to hundreds of layers). These dislocations are unstable with respect to the formation of focal conics [13], and turn into ''oily streaks'' which are well visible through the microscope [14]. In the region with a medium density of dislocations the typical distance between the dislocations is smaller

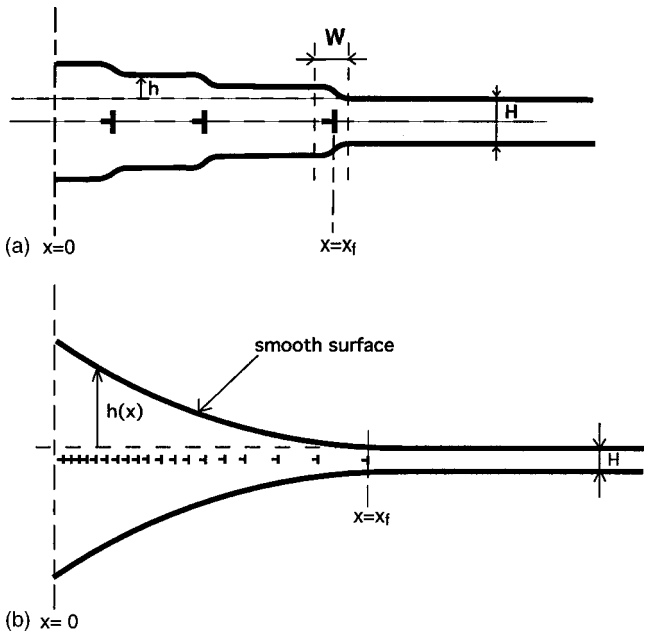

FIG. 2. (a) Meniscus in the vicinal regime. The dislocations are well separated. (b) Meniscus in the regime with medium density of dislocations. The distance Λ between two dislocations is smaller than the width W of the distortion produced by one dislocation at the surface. In this limit, the surface is smooth.

than the size of typical deformations at the surface induced by a single dislocation, but large enough to prevent the formation of giant dislocations and focal conics. This part of the meniscus was studied experimentally and theoretically in Ref. [2], but is described here theoretically in more detail. Finally, when the typical distance between dislocations becomes larger than the typical size of the deformation of the surface one enters the vicinal regime, which we discuss for the first time in this paper, to our knowledge. We emphasize that in the first region the energy of focal conics and the gravity play most probably important roles in the determination of the shape of the meniscus. In the second region, the surface tension, pressure difference, and energy of dislocations dominate, whereas in the third region (vicinal regime) entropic interactions between dislocations are important.

In the following, we describe the vicinal regime and the intermediate region with medium density of dislocations. Their spatial extensions are also estimated.

A. Vicinal regime

In this section we calculate the meniscus profile in the vicinal region, and in particular estimate its vertical size. For simplicity we will set the boundary conditions at the wall, neglecting for a moment the two regions of medium and high density of dislocations, and assuming that our vicinal region extends from the wall up to infinity. We find that the vertical size of the vicinal region is comparable to the smectic period d. It means that the vicinal region is so small that from the practical point of view it can be neglected, since it cannot be even observed in the experiments. Below we present a detailed discussion and calculations. At the matching point between the film and its meniscus, the distance between dislocations must diverge. As a consequence, there should exist a region where the dislocations are far apart from each other to be considered as independent [Fig. 2(a)]. This condition is fullfilled if the distance Λ between two neighboring dislocations is larger than the width W of the distorsion they produce at the free surface. According to Ref. [12], $W=2\sqrt{2\pi\lambda D}/f(\xi)$, where $D=H+2h$ is the total thickness [H is the thickness of the flat film, and $h(x)$ is the height of the meniscus above the flat film], $\lambda=\sqrt{K/B}$ is the smectic penetration length, and $f(\xi)$ is a function of the dimensionless parameter $\xi=(\gamma_{SA}-\sqrt{KB})/(\gamma_{SA}+\sqrt{KB})$. Function $f(\xi)$ varies from 1 to 0 when ξ varies from 0 to 1, but is always very close to 1 with usual values of K, B, and γ_{SA} in smectics (K is the bending modulus of the layers, and B their compressibility modulus). Thus condition

$$\Lambda \geqslant 2\sqrt{2\pi\lambda D} \tag{3.1a}$$

must be satisfied in the vicinal regime. In this case, the film surface is flat between two dislocations so that the excess of the surface free energy may be included in the self-energy of each dislocation. This way, the calculation of the shape of the meniscus is the same as in the theory of solids [15]. The main steps of the calculation are the following.

First of all, we assume that the Burgers vector b of each dislocation is equal to the layer thickness d, and that the total number of dislocations is fixed and given by $2h_0/d$, where $h_0=h(x=0)$ is the height of the meniscus at the wall. The surface energy is constant because the surface between the dislocations is flat.

Now the free energy associated with the dislocations must contain their self-energy and the interactions between the dislocations. There are two contributions to the dislocation interactions: one is entropic and one is elastic (via the deformations of the free surface). The former has the form $A/(x-x')^2$, where x and x' are the locations of two dislocations. The coefficient A depends on both the temperature and the energy E of the dislocations [15], and scales like $(k_BT)^2/E$. The latter decreases exponentially with the distance between the dislocations [8] [as $\exp-(x-x')^2$]. Numerical calculations show that elastic interactions are negligible with respect to entropic interactions (less than 10%) when $\Lambda=|x-x'|\geqslant 3W$. This condition, which reads

$$\Lambda \geqslant 6\sqrt{2\pi\lambda D}, \tag{3.1b}$$

is more restrictive than Eq. (3.1a). We assume it is satisfied in the vicinal regime. Finally, we assume that the interactions are restricted to the nearest neighbors. This way, the elastic energy of the system with N dislocations minus the energy of the system with zero dislocation per unit length is given by

$$F(x_i)=\sum_{i=2}^{N}\frac{A}{|x_i-x_{i-1}|^2}+EN+2(\gamma_{WS}-\gamma_{WA})h_0, \tag{3.2}$$

where x_i is the distance of the ith dislocation from the wall. The following surface tensions appear: γ_{SA}, γ_{WS}, and γ_{WA}, where W stands for the wall, S for the smectic, and A for the air. If the system is not connected to a reservoir of particles, then the volume of the meniscus is fixed, i.e.,

$$x_1 h_0 + \sum_{i=1}^{N-1} |x_{i+1} - x_i| h_i = \text{const}, \tag{3.3}$$

where $h_i = (N-i)d/2$ is the thickness of the meniscus between dislocations i and $i+1$. The shape of the meniscus is given by the locations x_i of the dislocations that minimize Eq. (3.2) with condition (3.3). In the continuous form (easier for calculations) the elastic energy is written as

$$F[h] = \int_0^{x_f} dx\, A(\rho(x))^3 + 2Eh_0/d + 2(\gamma_{WS} - \gamma_{WA})h_0, \tag{3.4}$$

where $\rho(x) = -(2/d)(dh/dx)$ is the density of dislocations per unit length, and $h(x)$ the height of the meniscus above the flat surface of the film. Condition (3.3) is now given by

$$2\int_0^{x_f} dx\, h(x) = \text{const}. \tag{3.5}$$

By taking condition (3.5) into account, minimization of Eq. (3.4) with respect to $h(x)$ gives

$$\frac{12A}{d^3}\frac{d}{dx}\left(\frac{dh}{dx}\right)^2 + \Delta p = 0. \tag{3.6}$$

The solution of Eq. (3.6) is

$$h(x) = a\left(\frac{x_f - x}{a}\right)^{3/2}, \tag{3.7}$$

where $a = 27A/(d^3 \Delta p)$ is a characteristic length. The length x_f and the difference $\Delta p = p_{\text{air}} - p_{\text{smectic}}$ between the air pressure and the pressure in the smectic are obtained from the boundary condition $h(x=0) = h_0$ and the condition of fixed volume [Eq. (3.5)].

In practice, Δp is fixed by the rest of the meniscus (which plays the role of a reservoir), while h_0 may be defined as the maximal height of the meniscus above which condition (3.1b) fails. With this definition, $h_0/(d/2)$ represents the maximal number of dislocations in the vicinal regime. Equations (3.7) and (3.1b) give, by assuming that $h_0 \ll H$,

$$\frac{h_0}{d/2} = \frac{1}{27\sqrt{2}} \frac{(k_B T)^2}{E d^{5/2} \lambda^{3/2}} \frac{1}{\Delta p m^{3/2}}, \tag{3.8}$$

where m is the number of layers in the free-standing film ($H = md$). With $d = 30$ Å, $\lambda = 10$ Å, and $E = 5 \times 10^{-7}$ dyn we calculate (in CGS units)

$$\frac{h_0}{d/2} = \frac{60}{\Delta p m^{3/2}}. \tag{3.9}$$

In typical experiments, $\Delta p \geq 100\ \text{dyn/cm}^2$ (see Sec. IV) and $m \geq 3$ which gives $h_0/(d/2) \leq 0.3$ (so $h_0 \ll H$, as we assumed above). This result shows that it does not make sense to speak about the vicinal regime in typical experiments, and that entropic interactions are negligible and always dominated by elastic and surface tension effects.

B. Region with a medium density of dislocations

According to the previous discussion, the dislocations are always so close to each other that they can never be considered as independent. Moreover, $\Lambda \ll 6\sqrt{2\pi\lambda D}$ in the region observable with an optical microscope. In this limit the dislocations can be replaced by a continuous distribution of infinitesimal dislocations along the x axis, so that the free surface is smooth at all scales [Fig. 2(b)]. This regime extends to the matching point with the film (at $x = x_f$), since the vicinal regime has a negligible extension, so we may set that $h = 0$ at point $x = x_f$. The energy of the system minus the energy of the system with $h(x) \equiv 0$ per unit length is then given by [2]

$$F[h(x)] = 2\gamma_{SA}\int_0^{x_f} dx\left(\sqrt{1 + (dh/dx)^2} - 1\right) + 2(\gamma_{WS} - \gamma_{WA})h_0 + 2\Delta p \int_0^{x_f} dx\, h(x) - \int_0^{x_f} dx\, E\frac{2}{d}\frac{dh}{dx}. \tag{3.10}$$

The first term corresponds to the excess of surface free energy in the limit of a continuous distribution of dislocations in the midle plane of the film; the second term (which is constant if h_0 is fixed) corresponds to the change of surface energy at the wall; the third term corresponds to the work of the pressure (Δp is the difference between the air pressure and the pressure in the smectic); and the fourth term describes the energy of the dislocations, that we assume to be proportional to their local density $\rho(x) = -(2/d)(dh/dx)$ and to some energy E. The important point here is that E does not depend explicitly on h and dh/dx, and corresponds to the core energy of the dislocations in the limit of a continuous distribution.

In the system there are two boundary conditions

$$h(x=0) = h_0 \tag{3.11}$$

and

$$\frac{dh}{dx}(x = x_f) = 0 \tag{3.12}$$

at point $x = x_f$, where the meniscus matches the smectic film. This condition is fulfilled if the interactions between the two free surfaces are negligible, which assumes that the film is thick enough (typically, its thickness must be more than 50 layers, a point we will discuss in a forthcoming publication). Another condition depends on whether the meniscus is coupled to a reservoir of particles or not. If there is no reservoir, then the total volume of the meniscus is fixed, and this gives rise to the additional condition, i.e.,

$$2\int_0^{x_f} dx\, h(x) = \text{const}. \tag{3.13}$$

With this condition, the point where $h(x) = 0$ (i.e., for $x = x_f$) and the pressure difference Δp depend on the volume. If the system is coupled to a reservoir of particles, Δp is

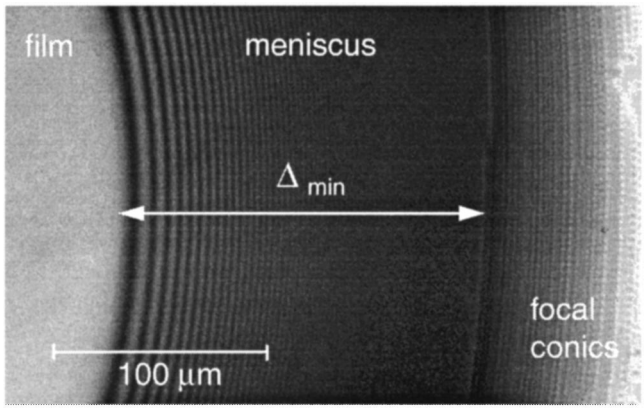

FIG. 3. Microscopic observation of a film and its meniscus, using both transmitted and reflected monochromatic light. The interference fringes observed in the thinnest part of the meniscus give the curvature radius of the meniscus ($R=2.8$ mm). Giant dislocations and chains of focal conics are visible in the thickest part of the meniscus. The distance Δ_{min} defines the part of the meniscus in which the dislocations are elementary.

given, which allows us to calculate the position x_f of the matching point and the volume of the meniscus.

The minimization of $f[h(x)]$ with respect to $h(x)$ gives the following equation for the profile $h(x)$:

$$\Delta p - \gamma_{SA}\frac{d}{dx}\left(\frac{dh/dx}{\sqrt{1+(dh/dx)^2}}\right)=0. \tag{3.14}$$

Please note that E does not appear in Eq. (3.14) due to the specific form of the energy term associated with dislocations. Also, the forces acting between the wall and the smectic do not appear in the boundary condition because the total height of the meniscus at the wall is supposed to be fixed by the number of dislocations.

The second term in Eq. (3.14) can be rewritten as

$$\gamma_{SA}\frac{(d^2h/dx^2)}{(1+(dh/dx)^2)^{3/2}}, \tag{3.15}$$

which is simply the curvature at point x multiplied by the surface tension. Thus Eq. (3.14) is nothing more than a Laplace law. Its solution is a circle of radius $R=(\Delta p/\gamma_{SA})$, i.e.,

$$h(x)=R-\sqrt{R^2-(x-x_f)^2}. \tag{3.16}$$

Finally we note that we have completely neglected the gravitational force, which is completely justified in usual experiments [$h_0 \ll l_c$, the gravitational capillary length defined in Eq. (1.1)]. In Appendix A, we describe the case of a meniscus near a cylindrical wall. Its shape resembles a catenoid, but its radial profile differs greatly from the circular one only when $\Delta p=0$. This case is not very pertinent experimentally, so we report the calculation in Appendix A.

All these descriptions (with a circular or a catenoid profile) are valid close to the film, as long as the density of dislocations is not too high. On the other hand, the experiment shows that giant dislocations parallel to the rim of the film nucleate in the thicker part of the meniscus (Fig. 3). These dislocations are rapidly unstable with respect to the formation of focal conics, and form strings of focal conics well visible in the thicker part of the meniscus. This phenomenon was explained by Boltenhagen, Lavrentovich, and Kléman [13]. The first dislocation that nucleates has a typical width of 1 μm in the transmission microscope, which corresponds to a Burgers vector of about 30 layers. The Burgers vector then systematically increases when the meniscus thickness increases. In Sec. III C, we discuss at which conditions giant dislocations may appear in the meniscus.

C. Formation of giant dislocations in the regime with a high density of dislocations

It is well known that in smectics, the dislocations tend to group together to form giant dislocations. This effect is due to the fact that in a bulk sample, the elastic energy of a dislocation is proportional to its Burgers vector. Then grouping n elementary dislocations together to form a giant dislocation of Burgers vector nd is energetically favorable, since it allows to reduce the core energy (one core instead of n). In confined geometry, the situation is more complicated because of the influence of the surfaces that limit the sample. In particular, the confinement effect and the interactions with the surfaces must be taken into account. This problem is solved when the smectic is confined between a plane and a sphere treated in homeotropic anchoring. In this case the elementary dislocations first group together two by two, then three by three, and so on, when the thickness of the sample (and so the density of dislocations) increases. This effect was observed experimentally both in thermotropic and lyotropic liquid crystals [16,17].

The situation is similar inside a meniscus apart from the fact that now, the two limiting surfaces are no longer solid but deformable. This difference is important and leads to a different behavior.

To analyze this problem, we first consider a circular meniscus of radius of curvature R much greater than h,

$$h(x)=\frac{1}{2R}(x_f-x)^2, \tag{3.17}$$

and we assume that all the dislocations are elementary [Fig. 4(a)]. We then consider a set of n dislocations at distance $\Delta=x_f-x$ from the rim of the film.

In which conditions is it energetically favorable to gather these dislocations [Fig. 4(b)]? To answer this question, we successively calculate the excess energy of the two configurations (with respect to the configuration with zero dislocation). For the first one (n elementary dislocation separated one from the other), we have

$$E_1=nE+n\gamma_{SA}\alpha d. \tag{3.18}$$

In this expression E is the energy of an elementary dislocation. It contains two contributions: the core energy E_c and an elastic energy proportional to d and equal to $(\sqrt{KB}/2)d$ (by assuming the core radius is equal to d) [18]. The second term in γ_{SA} corresponds to the excess of surface free energy due to the slope α of the free surface. This term is proportional to the slope square (because $nd=\alpha l$, where l is the distance covered by the n dislocations), and may be understood as the

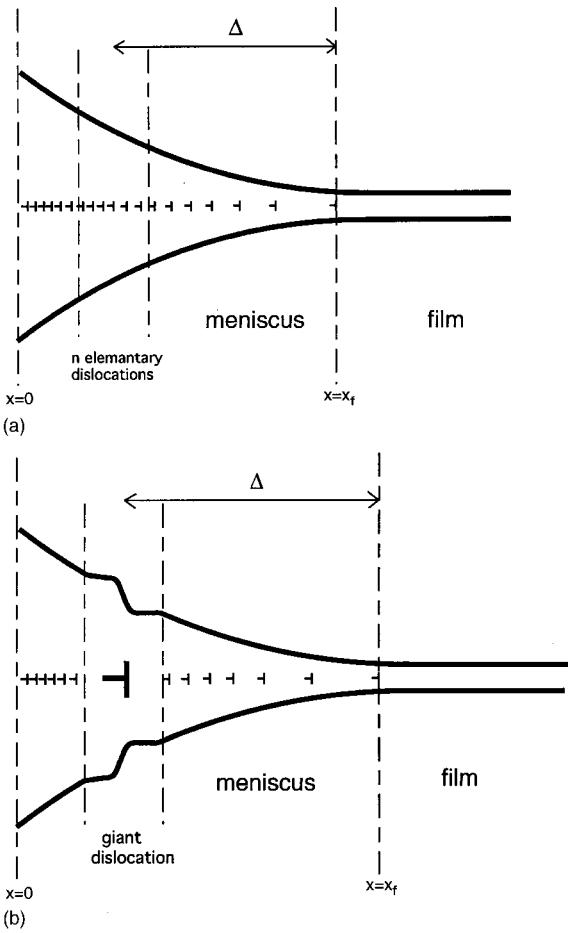

FIG. 4. Meniscus before (a) and after (b) the grouping of n elementary dislocations at a distance Δ from the edge of the film. Note that in (b) a giant dislocation has formed.

surface mediated interaction between dislocations. As at point $x, \alpha = \Delta/R$ (with $x_f - x = \Delta$), Eq. (3.18) becomes

$$E_1(n,\Delta) = nE_c + n\frac{\sqrt{KB}}{2}d + n\frac{\gamma_{SA}d}{2}\frac{\Delta}{R}. \qquad (3.19)$$

In the second configuration, n elementary dislocations are replaced by a dislocation of Burgers vector $b = nd$. For large n, it is reasonable to suppose that the dislocation splits into two wedge disclinations of ranks $\frac{1}{2}$ and $-\frac{1}{2}$. In this case, the dislocation energy contains four terms: the core energy of the two disclinations of the order of $2E_c$; the curvature energy of the layers of the 1/2 disclination, of the order of $(\pi K/2)\ln(n)$; the elastic energy outside the central zone of size nd, of the order of $(\sqrt{KB}/2)nd$, to which we must add a fourth term corresponding to the interaction energy with the free surfaces. This term has been calculated exactly [12], and equals $(B\lambda n^2 d^2/4\sqrt{\pi\lambda D})\mathrm{Li}_{1/2}(\xi)$, with $\lambda = \sqrt{K/B}$, $\xi = (\gamma_{SA} - \sqrt{KB})/(\gamma_{SA} + \sqrt{KB})$, $\mathrm{Li}_{1/2}(\xi) = \Sigma_{p=1}^{\infty}\xi^p(1/\sqrt{p})$, and $D \approx \Delta^2/R$, the total thickness at point $x_f - x = \Delta$ (by neglecting the film thickness). Collecting all the terms gives

$$E_2(n,\Delta) = 2E_c + \frac{\sqrt{KB}}{2}nd + \pi\frac{K}{2}\ln(n) + \frac{B\lambda n^2 d^2\sqrt{R}}{4\sqrt{\pi\lambda}\Delta}\mathrm{Li}_{1/2}(\xi). \qquad (3.20)$$

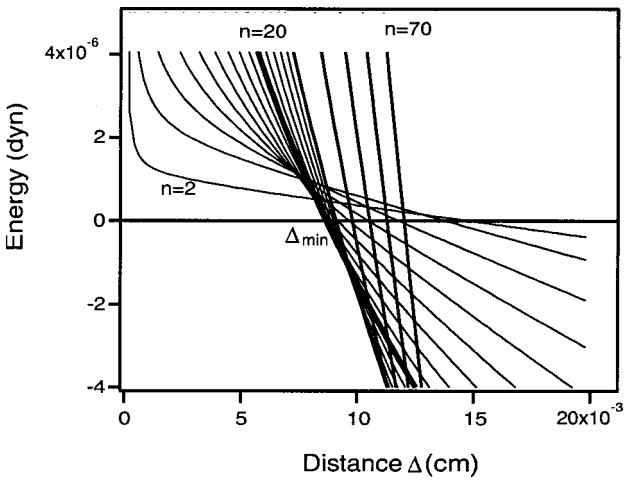

FIG. 5. Difference between the energy of a dislocation of the Burgers vector nd and the energy of n elementary dislocations as a function of the distance Δ from the edge of the film for different values of n. The increment of n between two thin curves is 2 and 10 between two thick lines. The value $\Delta_{\min}$ is the minimal distance below which grouping is unfavorable. At $\Delta_{\min}$ the first giant dislocation that forms has a Burgers vector of $20d$. This calculation was performed by choosing a 1-mm radius of the curvature of the meniscus.

In order to find under which condition a giant dislocation of Burgers vector nd may develop, in Fig. 5 we numerically plotted the difference $E_2 - E_1$ as a function of Δ for different values of n. To do this calculation, we have chosen $E_c = 0.1K$ (which is usual for a core energy in smectics [19]) and typical values for B, K, γ_{SA}, and R, namely, $B = 10^8\,\mathrm{erg/cm^3}$, $K = 10^{-6}\,\mathrm{dyn}$, $\gamma_{SA} = 25\,\mathrm{erg/cm^2}$, and $R = 1\,\mathrm{mm}$. Please note that in Eq. (3.20) ''the surface term'' decreases as $1/\Delta$, so that giant dislocations must appear in the thick part of the meniscus where Δ is large.

The graph in Fig. 5 shows that $\forall n \geqslant 2$, there exists a minimal distance $\Delta_{\min}$ below which the dislocations remain elementary. This limit unambiguously defines the regime with medium density of dislocations discussed before. Beyond this limit (i.e., in the thick part of the meniscus) giant dislocations tend to form. A surprising result shown by the numerical calculations is that at the distance $\Delta_{\min}$, the first grouping energetically favorable has a Burgers vector $b = n_{\min}d$ with $n_{\min} \neq 2$. For instance, for a curvature radius $R = 1$ mm we obtain $n_{\min} = 20$. This result is a consequence of the deformability of the free surface. The calculation also shows that the thicker the meniscus, the larger the Burgers vector of the giant dislocations should be. We also calculate the evolution of $\Delta_{\min}$ and $n_{\min}$ as a function of the curvature radius of the meniscus (Fig. 6). The results are that $\Delta_{\min}$ scales like R and that $n_{\min}$ does not change significantly.

These predictions are well verified experimentally. Indeed, microscope observation shows that the first giant dislocations have very large Burgers vectors [30 layers typically in Fig. 3, while the theory predicts 24 layers for $R = 2.8\,\mathrm{mm}$; see Fig. 6(b)]. The width of the circular regime (without giant dislocation) also increases when R increases, and is of the same order of magnitude as that we predict. For instance, we measure $\Delta_{\min} = 170\,\mu\mathrm{m}$ in Fig. 3, while Fig. 6(a) gives the theoretical value $\Delta_{\min} = 200\,\mu\mathrm{m}$ for $R = 2.8\,\mathrm{mm}$.

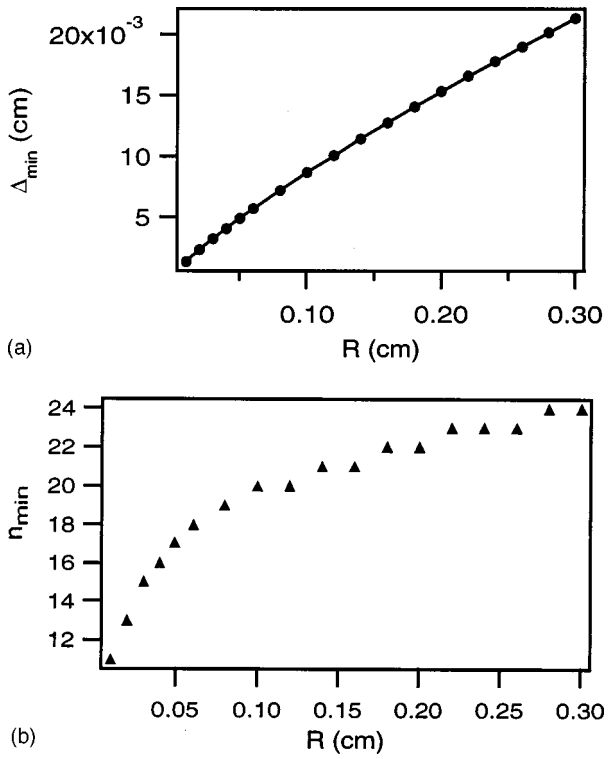

FIG. 6. (a) Minimal grouping distance as a function of the curvature radius of the meniscus. (b) Burgers vector $n_{\min}d$ of the giant dislocation at distance $\Delta_{\min}$ as a function of the curvature radius of the meniscus.

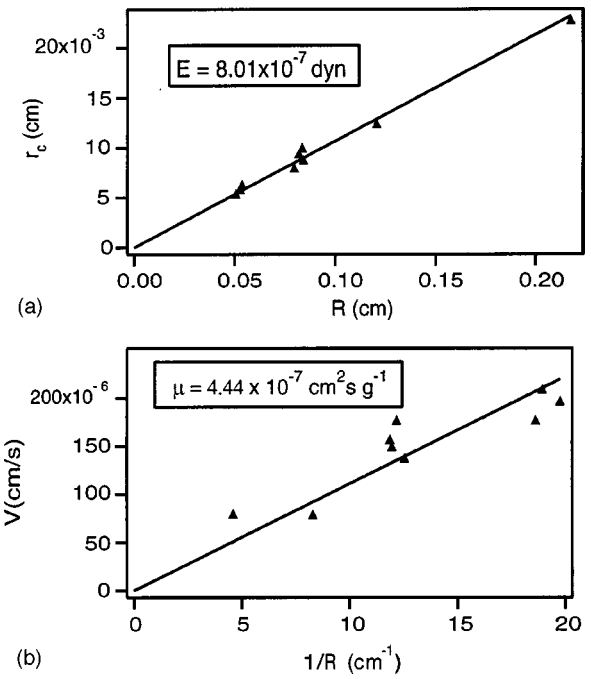

FIG. 7. (a) Critical radius of nucleation r_c as a function of the curvature radius of the meniscus R. (b) Velocity V of an elementary dislocation when its radius is much larger than r_c as a function of $1/R$.

In Sec. III, we propose an experiment to check the model of the meniscus in the case of fixed nonzero Δp. The experiment consists of nucleating a dislocation loop in the free-standing film, and of measuring its critical radius of nucleation and its mobility as a function of the radius of curvature of the meniscus in its circular part. These two quantities depend on the model of meniscus, and are compared to similar data deduced from two other experiments.

IV. NUCLEATION OF DISLOCATION LOOPS AND METASTABILITY OF SMECTIC FILMS

As we already mentioned in Sec. I, a smectic film is stable over many days (and even several months in an atmosphere without dust particles) in spite of the stress to which it is subjected. In practice, the pressure in the smectic is less than the air pressure, so that the film is homogeneously compressed over its whole surface. This stress σ exerts a Peach-Koehler force with magnitude σd on any dislocation of Burgers vector d in the film. This force tends to make the film thinner, and allows the fabrication of films with homogeneous thicknesses. In practice, there are many dislocations (forming arch textures [9]) in the films immediately after stretching. These dislocations progressively disappear by either annealing or moving to the meniscus. Usually, many hours are necessary to stabilize a film of constant thickness. In Ref. [2], we showed that it is then possible to remove the layers one by one by heating the film locally up to its transition temperature to the nematic phase. A very thin heating wire placed below the film is used to achieve the good condition of nucleation. The film is heated during a very short interval of time (1–2 ms), and then returns to its initial temperature (i.e., that of the oven) in a few ms. There are then two possibilities: either the loop radius is smaller than the critical radius of nucleation and it collapses, or the loop is larger and it grows to finally join the meniscus. Repeated measurements of the loop diameter as a function of time allows measurements of the critical radius of nucleation and the mobility of the dislocation. We recall that the critical radius of nucleation is simply given by $r_c = E/d\Delta p$, and that the mobility μ is defined to be $V = (\mu/d)f$, where f is the force acting on the dislocation and V its velocity. In the asymptotic regime, when the radius of the loop is much larger than r_c we have simply $V = \mu\Delta p$. We now need to know the pressure difference to calculate E and μ. According to the meniscus theory, Δp is given by the Laplace Law [Eq. (2.2)]. As a consequence, r_c and V are related to the radius of curvature R of the meniscus via the relations

$$r_c = \frac{E}{d\gamma_{SA}} R, \tag{4.1}$$

$$V = \mu \frac{\gamma_{SA}}{R}. \tag{4.2}$$

Thus the theory predicts that r_c is proportional to R and that the asymptotic velocity V is inversely proportional to R.

We performed systematic measurements by changing the radius of curvature of the meniscus by one order of magnitude. All the measurements were performed in thick films (more than 100 layers) of 8CB (octylcyanobiphenyl) at 28 °C. Our experimental results are displayed in Fig. 7. As expected we found that, within experimental errors, r_c is proportional to R and V is inversely proportional to R. We

deduce $E \approx 8 \times 10^{-7}$ dyn and $\mu \approx 4.4 \times 10^{-7}\ \mathrm{cm^2\,s\,g^{-1}}$. These two values are also in good agreement with those obtained from two other experiments that do not imply the meniscus model. Thus the line energy was obtained by measuring the deformation of a dislocation loop in a vertical film under the action of the gravity field [20]: it gives $E \approx 6 \times 10^{-7}$ dyn at 28 °C, in good agreement with the previous value. The mobility was obtained from a creep experiment. In this experiment we measured the viscoelastic response of a sample sandwiched between two glass plates treated in homeotropic anchoring and subjected to a sinusoidal deformation (see Appendix B for more details). It gives $\mu \approx 4.2 \times 10^{-7}\ \mathrm{cm^2\,s\,g^{-1}}$ in excellent agreement with that found in thick films. This again confirms that the pressure field is well given by the Laplace law in a smectic meniscus.

V. SUMMARY

The profile of a smectic meniscus is circular and not exponential as in usual liquids. It matches tangentially the film (when it is thick enough) which suggests that the vicinal regime with profile $x^{3/2}$ is very small. This result is confirmed by the theory, which shows that it does not make sense to speak about this regime in typical experiments. In the circular regime the dislocations are elementary, but so close to each other that the deformations they induce at the free surface strongly overlap. In this limit the free surface is smooth, and its excess of free energy may be calculated as in typical liquids. This observation leads to the typical Laplace law that gives the hydrostatic pressure in the meniscus. At equilibrium, the pressure is the same in the film as in the meniscus, so that the film is compressed. It turns out that the layers are elastic and can support this stress. This is the reason why it is possible to make stable films of variable thicknesses. It is also possible to change the pressure in the meniscus, by changing the volume of the smectic sample or the stretching velocity of the film during its preparation. This observation shows that the final state depends on the way the film has been created. We also checked experimentally that the Laplace law can be applied to smectic, by measuring both the critical radius of nucleation of a dislocation loop and the mobility of an elementary dislocation. Finally we have shown that elementary dislocations group together to form giant dislocations and chains of focal conic in the thick part of the meniscus. An interesting result is that the first ''giant'' dislocation to appear has a very large Burgers vector (typically 20 layers), which is different from what is observed between rigid surfaces where the dislocations group progressively two by two. We mention that when the film is very thin (less than 20 layers), the circular profile is no longer tangent to the film but makes an apparent angle that increases when the film thickness decreases. The present theory cannot explain this angle which is probably due to the disjoining pressure in the film. This effect will be described in a forthcoming publication.

ACKNOWLEDGMENTS

This work was supported in part by the KBN, Grant No. 2P03B12516, and by the European Research Network, Contract No. FMRX-CT96-0085. R.H. acknowledges with appreciation the support from CNRS and the Ministry of Education of France, and the hospitality of the Ecole Normale Supérieure de Lyon where a large part of this work was done.

APPENDIX A: CATENOID MENISCUS NEAR A CYLINDRICAL WALL

An unusual meniscus shape can be obtained near a cylindrical wall for $\Delta p = 0$. First, we will discuss it in the general case ($\Delta p \neq 0$). This situation occurs when a needle pierces the film [2]. We then show that when the system is coupled to a reservoir of particules ($\Delta p = 0$) the meniscus has a catenoid shape. Unfortunately the experimental realization of this case is beyond our reach.

Let us consider a cylindrical wall of radius r_0 with the smectic film around it. Let h be the height of the meniscus and r the distance from the center of the cylindrical wall. We assume that $h(r_0)$ is fixed and we define point r_1 by $h(r_1) = 0$. By analogy with Eq. (3.10), the total energy may be written in the form

$$\begin{aligned} F[h(r)] = {} & 2\gamma_{SA} \int_{r_0}^{r_1} 2\pi r\, dr \left(\sqrt{1+(dh/dr)^2} - 1\right) \\ & + 2(\gamma_{WS} - \gamma_{WA}) 2\pi r_0 h(r_0) \\ & + 2\Delta p \int_{r_0}^{r_1} 2\pi r\, dr\, h(r) \\ & - \int_{r_0}^{r_1} 2\pi r\, dr\, E \frac{2}{d} \frac{dh}{dr} + 2\pi r_1 E_1, \end{aligned} \tag{A1}$$

where we have added the term $2\pi r_1 E_1$ corresponding to some energy excess of the first dislocation in the meniscus. As we shall see later, this term is necessary to obtain a solution when $\Delta p = 0$. Minimization with respect to $h(r)$ gives

$$-r\Delta p - E/d + \gamma_{SA} \frac{d}{dr} \left(\frac{r\, dh/dr}{\sqrt{1+(dh/dr)^2}} \right) = 0 \tag{A2}$$

where Δp is set by the size of the meniscus (in the case of a fixed volume), or is zero when the film is coupled to a reservoir at the air pressure. Note that we have neglected the gravity force since the meniscus is small. Equation (A2) can be solved, but its full (and lengthy) analytical solution is not very instructive. Therefore, let us consider some limiting cases. For large r_0 and large Δp we obtain the circular meniscus studied in Sec. IV. This is true when $r_0 \Delta p \gg E/d$. Now let us consider the opposite case of a small meniscus [$h(r = r_0) = h_0$ is fixed and small with respect to the capillary length (1.1)] with $\Delta p = 0$, i.e., the meniscus is coupled to a reservoir of particles at the atmospheric pressure. In this case there are two terms in Eq. (A1): the term with the energy of dislocation, and the term with surface tension. It is easy to find that the dislocation term is rather small, i.e., $E/\gamma_{SA} d \approx 0.1$. For this reason we can treat the former as a perturbation.

Without the dislocations the meniscus would assume the shape of a minimal surface. A minimal surface is a surface whose area is minimal under the given boundary conditions.

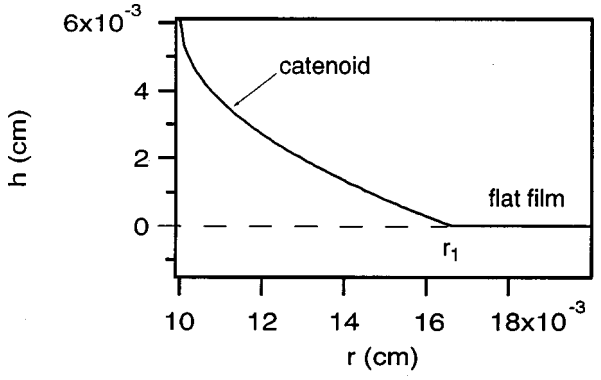

FIG. 8. Catenoid profile calculated from Eq. (B3) with $e=0.1$, $h_\infty=60\,\mu$m, and $r_\infty=100\,\mu$m. Note that the meniscus makes a nonzero angle with the film surface.

Here we have the surface that is spanned between two coaxial circles of radii r_0 (radius of the cylinder) and r_1 (the second radius). Such a surface is called a catenoid [21]. If we include the dislocations and expand the solution of Eq. (A2) in a small parameter $e=E/(\gamma_{SA}d)$, we find the following equation for the profile:

$$h(r)=h_\infty-r_\infty\ln[r/r_\infty+\sqrt{(r/r_\infty)^2-1}]-er_\infty\sqrt{(r/r_\infty)^2-1}, \tag{A3}$$

where r_∞ and h_∞ are integration constants that define the point of the surface with a vertical tangent. Of course the radius of the cylinder, r_0 is greater than r_∞. The first two terms give simply the catenoid and the last term is the small correction, since $e\approx 0.1$. This solution must satisfy boundary conditions $h(r=r_0)=h_0$, $h(r_1)=0$, and $2\gamma_{SA}[\cos(\theta)-1]-E_1/r_1=0$ at point $r=r_1$, with θ the contact angle between the meniscus and the flat film. This third condition that gives the force equilibrium at the edge of the meniscus is obtained by minimizing energy (A1) with respect to r_1, while keeping $h(r_1)=0$. It does not correspond to the zero contact angle, since at the point of contact the dislocation is not a straight line as in the case of flat wall, but has a circular shape. In other words the circular dislocation cannot wet the flat surface (Fig. 8). Thus the shape of the meniscus far away from the wall is mainly determined by the energy of dislocation, providing that the system is coupled to the reservoir of particles which give $\Delta p=0$. The conditions are sufficient to determine the constant r_∞, h_∞, and r_1.

APPENDIX B

In this appendix, we recall how the mobility of a dislocation can be deduced from a creep experiment. The experiment consists of imposing a sinusoidal deformation to a sample of 8CB sandwiched between two glass plates treated in homeotropic. The two plates make a small angle β that can be controlled with a very high accuracy (of the order of 10^{-4} rad). Because of this angle, an array of elementary edge dislocations form in the middle of the sample (because they are repelled from the two surfaces). In a good sample, these equilibrium dislocations are separated by distance d/β, and are the only dislocations that remain after recovery. The sample is placed in a dilation cell that is described in details in Ref. [22]. We just recall that the deformation is imposed

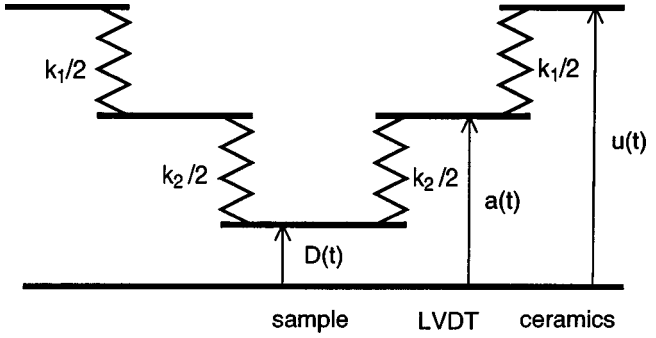

FIG. 9. Equivalent mechanical model for the dilation cell used to measure the mobility of the dislocations.

by three stacks of piezoelectrics through a rigid frame, and that the sample thickness D and the angle β are fixed with three differential screws. The temperature is stable within 0.01 °C. The deformation of the sample is measured with a LVDT (linear variable differential transformer) which is fixed on the oven close to the sample. It turns out that the cell is not infinitely rigid, and may be replaced by the equivalent mechanical model shown in Fig. 9. In this model, $u(t)$ is the displacement imposed by the ceramics, $a(t)$ is the displacement measured with the LVDT, and k_1 and k_2 are the force constants of the oven and the frame. Displacements $u(t)$ and $a(t)$, and their phase shift ϕ, are measured with a lock-in amplifier (Stanford SR850). The internal function generator of the lock-in amplifier is used to supply the ceramics. Sinusoidal deformations are used

$$u(t)=u_0\sin(\omega t), \tag{B1}$$

$$a(t)=a_0\sin(\omega t+\phi). \tag{B2}$$

At first, we take care that a_0 never exceeds 50 Å to avoid an undulation of the layers [23] and a helical instability of the screw dislocations [22,18]. In these conditions the only dislocations that contribute to the plastic deformation are the edge dislocations introduced by the misfit angle β. A calculation of the amplitude ratio a_0/u_0 and of the phase shift ϕ gives

$$\frac{a_0}{u_0}=\frac{\sqrt{[f_c^2+C(C+1)f^2]^2+f^2f_c^2}}{f_c^2+(1+C)^2f^2}, \tag{B3}$$

$$tg(\phi)=-\frac{ff_c}{f_c^2+(1+C)f^2}, \tag{B4}$$

where f is the frequency, C a dimensionless parameter

$$C=\frac{k_1}{k_2}+\frac{k_1D}{B}, \tag{B5}$$

and f_c a relaxation frequency

$$f_c=\frac{k_1\beta\mu}{2\pi}, \tag{B6}$$

which depends on the mobility of the dislocations. Measurements are performed at low frequency between 0.01 and 20 Hz (so that inertial effects can be neglected). Constants k_1

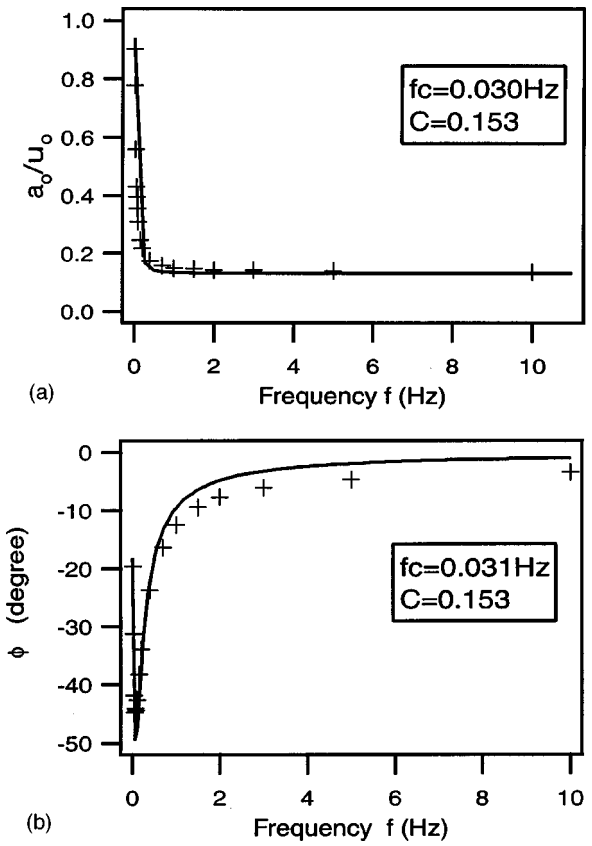

FIG. 10. (a) Ratio of the amplitudes measured (a_0) and imposed (u_0) as a function of the frequency. (b) Phase shift ϕ between the measured displacement (a) and the imposed displacement (u) as a function of the frequency.

and k_2 may be obtained by measuring the viscoelastic response of a silicon oil of known viscosity. This gives $k_1 = 8.9\times10^8$ dyn cm^{-3} and $k_1/k_2 = 0.097$. In Fig. 10 we show our experimental data for a sample of thickness $D = 100\,\mu$m and angle $\beta = 5\times10^{-4}$ rad. The best fit to Eqs. (B3) and (B4) gives $B = 1.6\times10^8$ erg/cm^3 and $\mu = 4.2\times10^{-7}$ cm^2 sg^{-1} at $T = 27\,^\circ$C. This value of the mobility is in excellent agreement with that found previously in thick smectic films.

We also measured the penetration length λ. To do this, we impose on the sample a sinusoidal modulation of increasing amplitude. The frequency chosen is much larger than the relaxation frequency. In practice, we performed our experiments in a 100-μm-thick sample between parallel glass plates ($\beta\approx10^{-4}$ rad) at $f = 20$ Hz, but we checked that the results were independent of the frequency above 5 Hz. In Fig. 11 we plot the amplitude a_0 and phase shift ϕ as functions of the displacement u_0 imposed by the ceramics.

As expected, the response is linear as long as $u_0 \leqslant u_0^c$ (elastic regime). In this regime, the phase shift ϕ is constant and close to zero (the dissipation is negligible), and

$$a_0 = \frac{C}{C+1}u_0. \tag{B7}$$

Thus measuring the slope gives B.

When $u_0 > u_0^c$, the curve a_0 vs u_0 shifts from the linear law. This behavior results from the undulation instability of

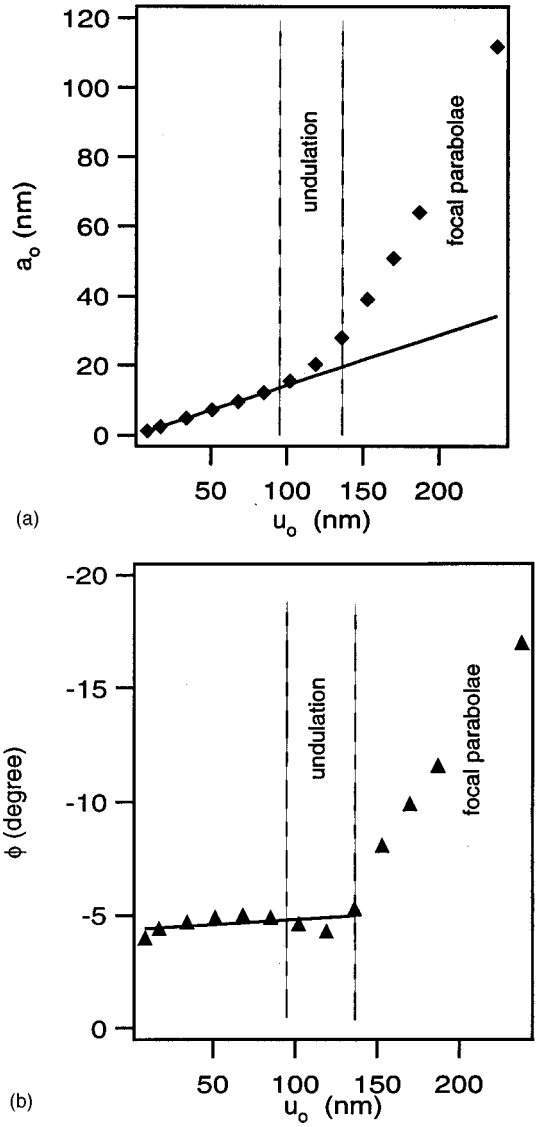

FIG. 11. (a) Measured displacement a_0 as a function of the imposed displacement u_0 at $f = 10$ Hz (the results are independent of the frequency between 10 and 50 Hz). (b) Phase shift ϕ as a function of u_0. It significantly increases when an array of focal parabolae nucleates.

the layers [23]. It is very well known that this instability develops (in 1 ms) when the sample thickness variation is more than $e_0^c = 2\pi\lambda$. Let a_0^c be the value of a_0 at the onset. According to our mechanical model, we have

$$e_0^c = a_0^c - \frac{k_1}{k_2}(u_0^c - a_0^c). \tag{B8}$$

This equation allows us to calculate λ. In 8CB at 28 °C, we found $\lambda\approx8$ Å. Note that the phase shift does not change significantly in the undulation regime, which means that the dissipation is negligible in this regime. The situation becomes different when $a_0 > 1.2a_0^c$. In this range of deformation, ϕ (and consequently the dissipation) strongly increases (Fig. 11). This effect is due to the nucleation of an array of parabolic focal conics [24]. These defects are clearly visible in the microscope.

[1] J. S. Rowlinson and B. Widom, *Molecular Theory of Capillarity* (Clarendon, Oxford, 1982).
[2] J-C. Géminard, R. Hołyst, and P. Oswald, Phys. Rev. Lett. **78**, 1924 (1997).
[3] O. D. Velev *et al.*, Phys. Rev. Lett. **75**, 264 (1995).
[4] J. Weertman and J. R. Weertman, *Elementary Dislocation Theory* (Oxford University Press, New York, 1992).
[5] F. C. Frank, Discuss. Faraday Soc. **25**, 1 (1958).
[6] P. G. de Gennes and J. Prost, *Physics of Liquid Crystals* (Clarendon, Oxford, 1993).
[7] M. Kléman, *Points, Lines and Walls* (Wiley, New York, 1983).
[8] R. Hołyst and P. Oswald, Int. J. Mod. Phys. B **9**, 1515 (1995).
[9] P. Pierański *et al.*, Physica A **194**, 364 (1993).
[10] C. Y. Young, R. Pindak, N. A. Clark, and R. B. Meyer, Phys. Rev. Lett. **40**, 773 (1978).
[11] C. Furtlehner and X. Leoncini, Stage de Magistère, Laboratoire de Physique des Solides, Université Paris-Sud, Orsay, 1991.
[12] L. Lejcek and P. Oswald, J. Phys. II **1**, 931 (1991); R. Hołyst, Phys. Rev. Lett. **72**, 4097 (1994).
[13] P. Boltenhagen, O. Lavrentovich, and M. Kléman, J. Phys. II **1**, 1233 (1991).
[14] J. E. Proust and E. Perez, J. Phys. (France) Lett. **38**, L-91 (1977).
[15] P. Nozières, in *Solids far from Equilibrium*, edited by C. Godrèche (Cambridge University Press, Cambridge, 1992), p. 1.
[16] R. Bartolino and G. Durand, Mol. Cryst. Liq. Cryst. **40**, 117 (1977).
[17] F. Nalet and J. Prost, Europhys. Lett. **4**, 307 (1987).
[18] M. Kléman, J. Phys. (France) **35**, 595 (1974).
[19] P. Oswald and M. Kléman, J. Phys. (France) Lett. **43**, L-411 (1982).
[20] J.-C. Géminard, C. Laroche, and P. Oswald, Phys. Rev. E **58**, 5923 (1998).
[21] See, for example, D. J. Struik, *Lectures on Classical Differential Geometry* (Dover, New York, 1950).
[22] P. Oswald and D. Lefur, C. R. Seances Acad. Sci., Ser. 2 **297**, 699 (1983).
[23] R. Ribotta and G. Durand, J. Phys. (France) **38**, 179 (1977).
[24] Ch. S. Rosenblatt, R. Pindak, N. A. Clark, and R. B. Meyer, J. Phys. (France) **38**, 1105 (1977).